Myocardial infarction and remodeling in mice: effect of reperfusion

LLOYD H. MICHAEL,[1] CHRISTIE M. BALLANTYNE,[1] JUSTIN P. ZACHARIAH,[1] KENNETH E. GOULD,[2] JENNIFER S. POCIUS,[1] GEORGE E. TAFFET,[1] CRAIG J. HARTLEY,[1] THUY T. PHAM,[1] SHERITA L. DANIEL,[1] ETAI FUNK,[1] AND MARK L. ENTMAN[1]

[1]*DeBakey Heart Center and Department of Medicine, Baylor College of Medicine, Houston, Texas 77030-3498; and* [2]*Lilly Research Laboratories, Eli Lilly and Company, Indianapolis, Indiana 46285*

Michael, Lloyd H., Christie M. Ballantyne, Justin P. Zachariah, Kenneth E. Gould, Jennifer S. Pocius, George E. Taffet, Craig J. Hartley, Thuy T. Pham, Sherita L. Daniel, Etai Funk, and Mark L. Entman. Myocardial infarction and remodeling in mice: effect of reperfusion. *Am. J. Physiol.* 277 (*Heart Circ. Physiol.* 46): H660–H668, 1999.—Anatomic and functional changes after either a permanent left anterior descending coronary artery occlusion (PO) or 2 h of occlusion followed by reperfusion (OR) in C57BL/6 mice were examined and compared with those in sham-operated mice. Both interventions generated infarcts comprising 30% of the left ventricle (LV) measured at 24 h and equivalent suppression of LV ejection velocity and filling velocity measured by Doppler ultrasound at 1 wk. Serial follow-up revealed that the ventricular ejection velocity and filling velocity returned to the levels of the sham-operated controls in the OR group at 2 wk and remained there; in contrast, PO animals continued to display suppression of both systolic and diastolic function. In contrast, ejection fractions of PO and OR animals were depressed equivalently (50% from sham-operated controls). Anatomic reconstruction of serial cross sections revealed that the percentage of the LV endocardial area overlying the ventricular scar (expansion ratio) was significantly larger in the PO group vs. the OR group (18 ± 1.7% vs. 12 ± 0.9%, $P < 0.05$). The septum that was never involved in the infarction had a significantly ($P < 0.002$) increased mass in PO animals (22.5 ± 1.08 mg) vs. OR (17.8 ± 1.10 mg) or sham control (14.8 ± 0.99 mg) animals. Regression analysis demonstrated that the extent of septal hypertrophy correlated with LV expansion ratio. Thus late reperfusion appears to reduce the degree of infarct expansion even under circumstances in which it no longer can alter infarct size. We suggest that reperfusion promoted more effective ventricular repair, less infarct expansion, and significant recovery or preservation of ventricular function.

coronary artery occlusion; nuclear imaging; hypertrophy; systolic and diastolic function; ejection fraction

ALTHOUGH REDUCING THE AMOUNT of infarcted myocardium remains a primary goal of treatment for acute myocardial infarction, substantial evidence has accumulated suggesting that the efficiency and quality of tissue repair also play an important part in determining long-term ventricular function and mortality after infarction (32). Among the interventions designed to promote more effective tissue repair, the earliest data were associated with reduction of cardiac afterload and ventricular work. The use of angiotensin-converting enzyme (ACE) inhibitors has now become standard therapy for treatment of large transmural myocardial infarctions. More recently, it has been demonstrated that ACE inhibitors may also favorably influence tissue repair by direct inhibition of localized renin-angiotensin systems in the heart (39).

Over the same historical period, reperfusion of the previously occluded coronary vessel became the standard therapy to reduce tissue injury. Initially, the focus of this effort was to open the coronary artery in an attempt to decrease the degree of infarction. In subsequent studies, however, it also became apparent that reperfusion, even instituted later when tissue infarction could no longer be reduced, effectively promoted tissue repair (15). The combination of an open vessel and the possibility for promoting more effective tissue repair by pharmacological intervention led to a variety of studies assessing factors that play critical roles in tissue repair. It is hoped that methods of augmenting tissue repair will follow.

One of the effects of reperfusion of the infarcted myocardium is an accelerated inflammatory reaction (5) that, under certain circumstances, can actually extend injury (6). However, substantial evidence suggests that leukocyte influx into the previously infarcted area may help promote tissue repair (28) by enhancing phagocytosis (3, 34) as well as production of growth factors and cytokines that may modulate scar formation and angiogenesis (9, 36). Our laboratory and others (1, 21) have described the early influx of monocytes into the infarct area on reperfusion.

Studies in larger animals that describe the cellular and molecular events associated with tissue repair and scar formation are inevitably limited by the ability to deduce the relative importance of the factors described. Treatment with neutralizing monoclonal antibodies over several weeks, even if such antibodies were available, would be of enormous expense and doubtful practicality. For this reason, our laboratory has produced models of chronic myocardial infarction in mice (27). Infarction is created by permanent coronary artery occlusion or by occlusion for a period of 1–2 h, after which the occlusion is removed and coronary flow to the myocardium is restored. These models allow use of genetic modification strategies in the study of the molecular and cellular events associated with the reaction to injury. The models yield mice capable of surviving for long periods after infarction and allow hemodynamic measurements. The purpose of the current study was to characterize repair in mice with myocardial

The costs of publication of this article were defrayed in part by the payment of page charges. The article must therefore be hereby marked "*advertisement*" in accordance with 18 U.S.C. Section 1734 solely to indicate this fact.

infarction and to define the effects of reperfusion on ventricular remodeling and systolic and diastolic function. The results suggest that, in the absence of reperfusion, infarcts of equivalent size undergo greater expansion that can be directly related to greater ventricular hypertrophy. These anatomic features of remodeling are associated with decreased systolic and diastolic function.

METHODS

Infarct and reperfusion model. Male C57BL/6 mice 12–16 wk of age (22.5–30.5 g body wt) were obtained from Harlan Sprague Dawley (Houston, TX). All animal protocols were approved by the Institutional Animal Care and Use Committees of the American Association for Accreditation of Laboratory Animal Care-accredited institutions Baylor College of Medicine and Lilly Research Laboratories, in accordance with the National Institutes of Health (NIH) *Guide for the Care and Use of Laboratory Animals* [DHHS Publication No. (NIH) 85–23, Revised 1985, Office of Science and Health Reports, Bethesda, MD 20892]. The following brief description is excerpted from a more detailed account (27). Anesthesia was produced by an intraperitoneal injection of pentobarbital sodium (4 mg/ml; 10 μl/g body wt). Mice were placed in a supine position with paws taped to the operating table. With direct visualization of the trachea, an endotracheal tube was inserted and connected to a Harvard rodent volume-cycled ventilator cycling at 100 min^{-1} with volume sufficient to adequately expand the lungs but not overexpand. The inflow valve was supplied with 100% oxygen.

For studies of the myocardial response to permanent occlusion, ligation of the anterior descending branch of the left coronary artery was achieved by tying 8-0 silk suture around the artery. The suture was passed under the artery at a position ~1 mm from the tip of the normally positioned left auricle.

For studies of the effect of reperfusion after coronary artery occlusion, the ligature was tied at the same location on the coronary artery used for the permanent occlusion. However, to allow subsequent reestablishment of blood flow, occlusion was produced by placing a 1-mm length of polyethylene (PE) tubing (OD = 0.61 mm; Intramedic PE-10, Clay Adams, Parsippany, NJ) on the artery and fixing it in place with the ligature. The artery was then compressed by tightening the ligature, producing myocardial blanching and electrocardiographic (ECG) S-T segment elevation as observed in permanent ligations (27). After occlusion for the desired time, blood flow was restored by removing the ligature and PE tubing. The chest wall was then closed by a 6-0 Ticron suture with one layer through the chest wall and muscle and a second layer through the skin and subcutaneous layer.

After surgical closing of the chest, the endotracheal tube was removed, warmth was provided by a heat lamp, and 100% oxygen was provided via a nasal cone. The animal was given 0.1 mg/kg butorphanol tartrate as an analgesic, and it became sternally recumbent within 1 h. After surviving the experimental infarct the mice recovered, and this allowed postoperative physiological measurement. Sham-operated mice underwent an identical procedure with placement of the ligature but did not undergo coronary artery occlusion.

Doppler ultrasound measurements. Mice were anesthetized by an intraperitoneal injection of a mixture (acepromazine 1.4 mg/ml, xylazine 8.6 mg/ml, and ketamine 42.8 mg/ml) at a dose of 0.5 μl/g body wt. They were taped to a temperature-controlled laminated plastic board with copper electrodes placed such that the three bipolar limb leads allowed ECG monitoring. Body fur at the left lower sternal border was clipped lightly, and the skin in that area was wetted with warm water to improve sound transmission. A 10-MHz pulsed Doppler probe was positioned at the xiphoid process of the sternum with minimal pressure. The pulsed Doppler range gate depth was set at 4–7 mm to obtain optimal signals from the left ventricular (LV) inflow and outflow tracks substernally as previously described (12, 13). An ECG timing signal was superimposed on the Doppler display using an R wave trigger. Repeated measures were made from each animal to allow for observation at different heart rates and to ascertain the reproducibility of the measurements. For each study, four to six beats were analyzed. The pulsed Doppler instrument and probes were custom made in our laboratories (13), and the Doppler audio signals were processed by a Medasonics (Vasculab SP-25A) spectrum analyzer for subsequent analysis on personal computer using NIH Image. In later studies, the Doppler signals were processed by a high-speed spectrum analyzer and software (Indus Instruments, Houston, TX) specifically optimized for use with mice. In each case the observer was blinded to the experimental conditions. Data were quantified in a Lotus 1–2–3 spreadsheet. Mice were allowed to recover and were followed sequentially, comparing pre- and postprocedure measurements in the same mouse. No deaths were caused by anesthesia in preocclusion or postocclusion Doppler studies.

Ventricular ejection fraction by cardiac nuclear imaging. For murine imaging a multiwire gamma camera (10) optimized for use with ^{178}Ta was fitted with a 2-mm-diameter pin-hole lens to project an enlarged image of the mouse heart on the image plane at a frame rate of 160 s^{-1} (Proportional Technologies, Houston, TX). ^{178}Ta with a half-life ($T½$) of 9.3 min was generated and concentrated on site as needed from ^{178}W ($T½$ = 21.7 days). The short $T½$ allowed concentration of high radiation doses (20 mCi) in a very small volume (10 μl) to maintain image quality and sequential individual studies timed ~30 min apart.

Mice were anesthetized with 0.2–0.4 ml of pentobarbital sodium solution (4 mg/ml) given intraperitoneally and were taped supine to a small plastic board with ECG electrodes under each limb. An intravenous catheter (PE-10 tubing) was placed in the jugular vein for injection of a bolus containing 20 mCi of ^{178}Ta in 10 μl of 0.1 M HCl followed by 10 μl of normal saline. After injection, images were taken for 7.5 s at 160 frames/s and then stored and analyzed by software originally designed and validated for human cardiac imaging (44). For assessment of ejection fraction, right ventricular (RV) and LV beats were identified, background radiation was subtracted, and 16-frame cine loops of both the RV and LV cavities were produced. Ejection fraction was calculated from the total counts in end-systolic and end-diastolic frames, which has been shown to be proportional to LV blood volume.

Assessment of area at risk and infarct size. At 24 h after coronary artery occlusion or occlusion-reperfusion event, hearts were removed and area at risk and infarct size were measured as previously described (27). Briefly, hearts were removed after euthanasia by intravenous injection of 50 mM KCl, 5 mM EGTA, and 10 U/ml heparin. The aorta was cannulated with a 22-gauge Luer stub, and 50 μl of 1% Evans blue were perfused into the aorta and coronary arteries with distribution throughout the ventricular wall proximal to the site of coronary artery ligation. The transverse section cutter used in these studies had blades spaced 1,000 μm apart; therefore, each heart section between the blades had section thicknesses of 1,000 μm, whereas the apical tip and base may vary outside these thicknesses because the first cutter blade was positioned at the site of coronary artery occlusion. In the

typical 12- to 16-wk-old mouse, this cutting gave three equal 1,000-μm-thick pieces, an ~2,000-μm-thick basal section, and an apical section generally <1,000 μm thick.

After staining with 1.5% 2,3,5-triphenyltetrazolium chloride and image analysis, the infarction was determined by the following equations. Weight of infarction is $(A_1 \times W_1) + (A_2 \times W_2) + (A_3 \times W_3) + (A_4 \times W_4) + (A_5 \times W_5)$, where A is percent area of infarction by planimetry from subscripted numbers 1–5 representing sections and W is weight of the same numbered sections. Percentage of infarcted LV is (W of infarction/W of LV) × 100. Area at risk as percentage of LV was calculated by (W of LV − W of LV stained blue) × W of LV. The weight of LV stained blue was calculated in a similar fashion by the sum of products of the percent area of each slice times the weight of the respective slice.

Perfusion fixation and histology. For assessment of changes in cardiac structure, the intravenous cardioplegic solution contained (in g/l) 4.0 NaCl, 3.7 KCl, 1.0 $NaHCO_3$, 2.0 glucose, 3.0 2,3-butanedione monoxime, 3.8 EGTA, and 0.0002 nifedipine. This solution was perfused through the jugular vein to promote quiescence and relaxation. After being excised and rinsed in cold cardioplegic solution, the aorta was cannulated with a 22-gauge blunt needle and the left atrial appendage with a PE-50 catheter pushed across the mitral valve into the LV and secured in place. Hearts were fixed for 10 min by aortic perfusion of 10% zinc-buffered Formalin with the LV drain held vertically 16 cm above the base of the heart to maintain constant LV pressure at ~16 cmH_2O. After the cannulas were removed, fixation by immersion continued for 2 h, after which the hearts were dehydrated, cleared, and embedded in paraffin. The entire heart was cross-sectioned into 5-μm sections from base to apex (see Fig. 1). Sections were stained with hematoxylin and eosin or Masson trichrome stain.

Analysis of ventricular mass and scar formation. The mass of the LV and septum was obtained by integration of a curve created by plotting the LV area measured in each cross section against the distance of the cross section from the base of the heart (see Fig. 1). The basal cross section used as the starting point in each heart was identified as the last cross section containing any part of the aortic valve and every 50th cross section (intervals of 5 μm × 50 = 250 μm) was analyzed. The sum of the areas in each of the partitions was obtained by integration of this curve that was carried out by dividing the interval of integration (x-axis) into 250-μm partitions representing each of the cross sections, beginning at the first basal cross section and ending at the last apical cross section. The sum was then used as an estimate of total ventricular space occupied by the myocardium in each heart. LV myocardial mass was derived from this space estimate by multiplying by the commonly assumed muscle tissue density of 1.065 mg/μl. The mass of the interventricular septum was separately analyzed using identical methods. In the latter case, the LV septum was described in the first basal section and continued through the last section to show evidence of the RV chamber. The edges of the septum were defined by the approximate sites of the anterior and posterior interventricular (longitudinal) sulci on each cross section. The actual line of demarcation was arbitrarily drawn on each section with consideration of the sites of these sulci and with the understanding of a slight rightward (toward RV) convexity of the interventricular septum.

Computation of ventricular expansion ratio. In each cardiac cross section, a thin segment was identified in the LV free

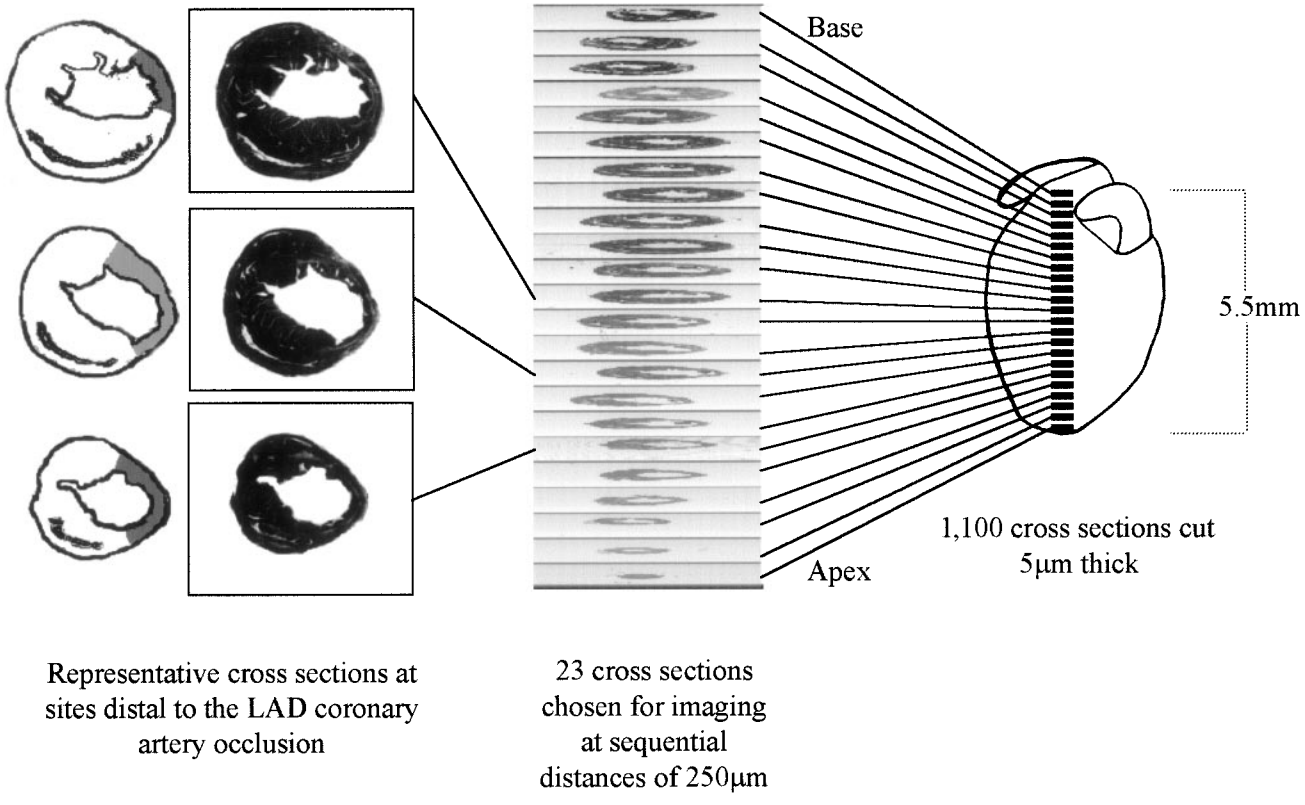

Fig. 1. Representative mouse heart imaging schematic illustrating that a 5.5-mm heart is cross-sectioned into 1,100 5-μm-thick sections, from which 23 are chosen for analysis of ventricular mass and dimension. LAD, left anterior descending coronary artery.

wall. The thickness of these segments was characteristically <40% of the remaining ventricular free wall in the cross section. The thickness of thin segments varied <10% when compared in all of the cross sections from a single heart. The length of the endocardial surface underlying each thin segment was measured as well as the length of the total endocardial surface in the cross section. Thin segment length and total endocardial surface length were plotted against the distance of the cross section from the base of the heart. (see RESULTS). Each plot was integrated by dividing the interval of integration (*x*-axis) into 250-μm partitions representing the distance between the cross sections taken for analysis, beginning at the first basal cross section and ending at the last apical cross section, and obtaining the sum of the areas in each of the partitions. The sums were used as estimates for the thin segment area and for the total endocardial surface area in the LV of each heart. The ventricular expansion ratio was calculated by dividing thin segment endocardial area by total endocardial area and multiplying by 100.

Statistics. Differences between groups were determined using analysis of variance. Specific group differences were determined using an unpaired *t*-test with Dunnett's correction for multiple comparisons. The data not representing normal distribution were tested by nonparametric rank-sum tests. Correlation between variables was tested by linear regression analysis. Values listed are means ± SE. For all testing, $P < 0.05$ was used to determine significance.

RESULTS

A total of 35 mice successfully completed the 24-h infarct size protocol, which represented 95% survival for sham, 75% for permanent occlusion, and 60% for occlusion-reperfusion mice. The hemodynamic assessment with ultrasound and nuclear imaging and the ventricular dimension experiments necessitated an additional 22 sham, 32 permanent occlusion, and 24 occlusion-reperfusion mice; this represented survival averaging 92% for sham, 60% for permanent occlusion, and 45% for occlusion-reperfusion mice.

Infarct size. Our laboratories have used a coronary occlusion site on the mouse that results in an infarction of ~30% of the LV (27). Mice reperfused after 30 and 60 min of occlusion demonstrated significantly reduced myocardial infarct size compared with permanent occlusion mice. In the current study, we examined and compared tissue repair under conditions of identical infarct size. In reperfused mice, we measured infarct size as a function of occlusion time with the intent to determine the time of reperfusion that would not result in a significant reduction in myocardial infarct size. When the coronary artery was occluded for 120 min, myocardial infarct size was identical to that seen with a permanent occlusion, resulting in an infarct of 30% of the LV, representing ~65% of the area at risk (Fig. 2). The remainder of the study, therefore, compared hemodynamic and anatomic consequences of a permanent occlusion with those of an occlusion of 2 h followed by reperfusion.

Hemodynamic function. Using a nuclear imaging camera developed in our laboratory (10), we were able to measure ejection fractions in mice at various times after permanent occlusion or reperfusion. As previously described (11), acute occlusion of the coronary vessel

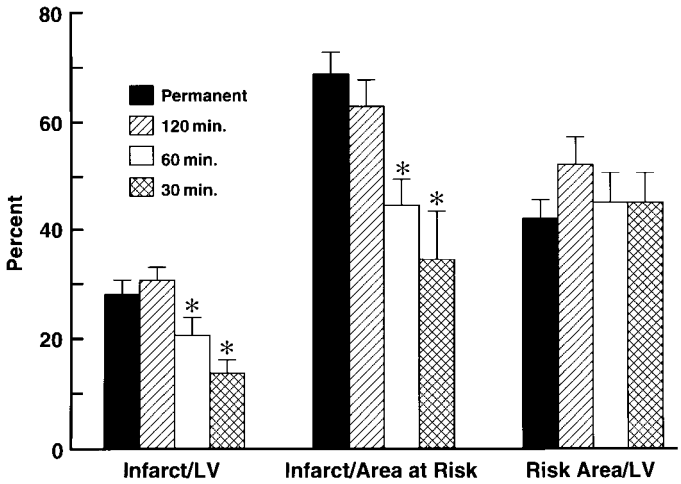

Fig. 2. Infarct size and area at risk after LAD occlusions of 30 ($n = 5$), 60 ($n = 7$), and 120 ($n = 10$) min followed by reperfusion or permanent LAD occlusion ($n = 13$). Hearts were removed at autopsy 24 h after occlusion. Data for permanent occlusion and 30- and 60-min occlusion followed by reperfusion are from Ref. 27. Values are means ± SE. *$P < 0.05$ vs. permanent occlusion. LV, left ventricle.

reduces ejection fractions to values commonly below 30%. The ejection fractions after permanent occlusion or occlusion and reperfusion appeared to be stable from 2 wk to several months after infarct and therefore were combined. The ejection fraction was 26.4 ± 3.1% ($n = 23$) for mice with permanent occlusions and was almost identical (24.1 ± 4.0%; $n = 10$) for the reperfused group; sham-operated mice had significantly higher ejection fractions of 47 ± 2.8% ($n = 10$; $P < 0.05$). Representative end-diastolic and end-systolic images from a normal, nonoperated mouse and a mouse with a permanent coronary artery occlusion are shown in Fig. 3. In this example, the ejection fractions are 60% in the normal mouse and 17% in the mouse with the permanent occlusion. The resolution of the images was sufficient to appreciate the dilated and poorly contracting infarcted cardiac apex compared with the motion of the same region in the normal mouse and to recognize the heterogeneity in wall motion within a given ventricle.

In contrast, when pulsed Doppler measurements of peak aortic flow velocity (Fig. 4*A*) and average aortic flow velocity (Fig. 4*B*) were compared, there were

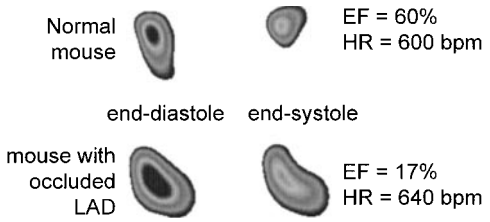

Fig. 3. First-pass nuclear images of LV blood pool taken at end diastole and at end systole from a normal mouse and from a mouse with a permanent LAD occlusion. Images were taken with multiwire gamma camera fitted with a 2-mm pin-hole lens at a rate of 160 frames/s. ^{178}Ta was concentrated to 20 mCi in 10 μl of fluid, injected as a bolus into jugular vein, and flushed with 10 μl of 0.9% NaCl. Occluded mouse has a larger ventricular cavity with reduced ejection fraction (EF) and with dilatation and paradoxical wall motion at apex. HR, heart rate; bpm, beats per minute.

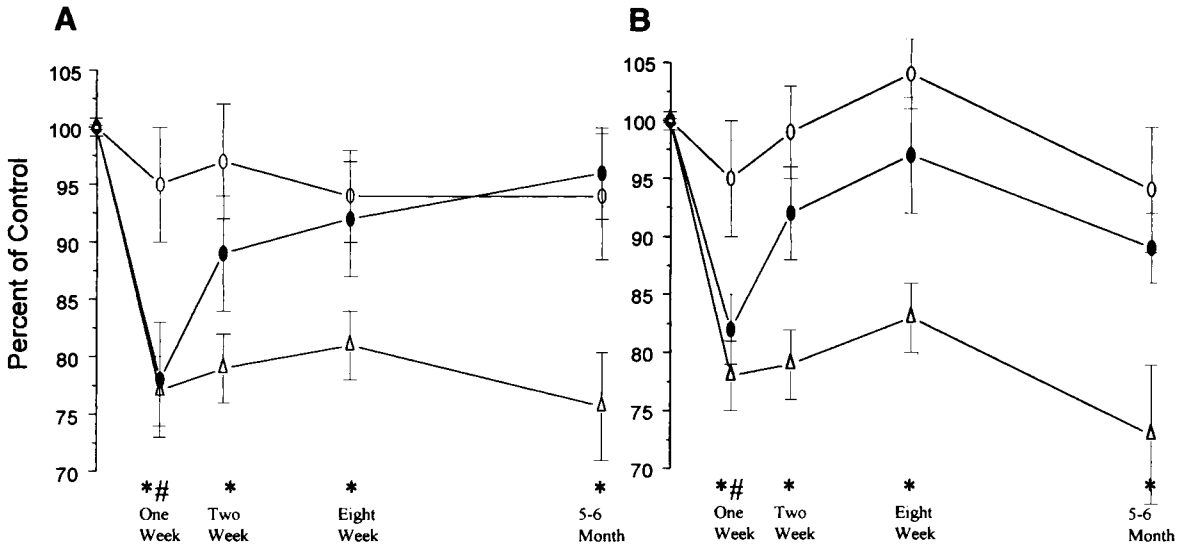

Fig. 4. *A*: peak aortic flow velocity followed for 5–6 mo in mice subjected to sham operation (○), 2-h occlusion followed by reperfusion (●), and permanent occlusion (△). Data are % of preoperative values and are expressed as means ± SE. Preoperative values: sham (n = 15), 104 ± 20 cm/s; permanent occlusion (n = 24), 111 ± 17 cm/s; reperfusion (n = 13), 102 ± 10 cm/s. *$P < 0.05$, permanent occlusion vs. sham; #$P < 0.05$, reperfusion vs. sham. *B*: average aortic flow velocity followed for 5–6 mo in mice subjected to sham operation, 2 h of ischemia followed by reperfusion, and permanent occlusion. Data are % of preoperative values and are expressed as means ± SE. Preoperative values: sham (n = 15), 74 ± 16.9 cm/s; permanent occlusion (n = 24), 81 ± 15.0 cm/s; reperfusion (n = 13), 69 ± 5.9 cm/s. *$P < 0.05$, permanent occlusion vs. sham; #$P < 0.05$, reperfusion vs. sham.

significant differences in systolic function between mice with permanent coronary occlusions and reperfused mice. The mice with permanent occlusions showed significant reduction in both aortic flow velocities, which persisted throughout the 5- to 6-mo examination period ($P < 0.05$ vs. reperfused group). Although these flow velocity parameters were decreased to a similar extent at 1 wk in the reperfusion group, recovery of function to preocclusion levels occurred by 2 wk. These data suggest that the reperfused mice were more capable of compensating for the cardiac injury.

Diastolic filling was also evaluated. In our previous work (41) we described methods for analyzing transmitral blood flow velocity in the LV by measuring the early peak rapid filling velocity (E) and the atrial filling velocity (A) during diastole. We confirmed the strong dependence of the ratio E/A on heart rate and the relative independence of E. We therefore confined our analysis to E (Fig. 5). At 1 and 2 wk after infarction, E of the sham-operated mice and all infarcted mice was reduced slightly to ~80–90% of preocclusion values. E of the sham-operated and reperfused animals remained at that level throughout the 5–6 mo of observation. In contrast, E of the permanently occluded animals continued to fall, reaching 77% of the preocclusion value by the eighth week ($P < 0.05$ vs. sham) and remaining at this level throughout the 5- to 6-mo observation period. Differences in the ventricular repair and healing processes are likely causes for divergence in systolic and diastolic function caused by permanent occlusion and reperfusion infarcts of similar size.

Ventricular dimensions. We characterized the anatomic changes associated with tissue repair and adaptation to the injury. LV from sham-operated and infarcted mice were examined over the period from 2 to 14 mo after infarct. This was the period during which the postinfarct functional changes in both systolic and diastolic parameters remained stable and clearly distinguished mice reperfused after coronary occlusion from those in which the occlusion was permanent. Our intent was to characterize the anatomic counterparts of these differences.

In cross sections from each mouse heart, the area of infarction was represented by a thinned segment of ventricular free wall containing both scar and scattered

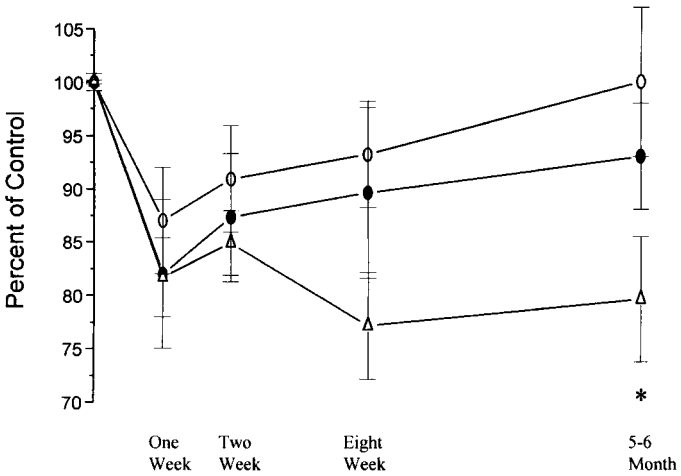

Fig. 5. Peak early filling velocity followed for 5–6 mo in mice subjected to sham operation (○), 2-h ischemia followed by reperfusion (●), and permanent occlusion (△). Data are % of preoperative values and are expressed as means ± SE. Preoperative values: sham (n = 15), 69 ± 3.1 cm/s; permanent occlusion (n = 24), 71 ± 1.9 cm/s; reperfusion (n = 13) 66 ± 2.1 cm/s. *$P < 0.05$ vs. sham.

Fig. 6. Cross sections of representative mouse hearts at 5 sites (basal to distal) illustrating appearance of sham, permanent occlusion, and occlusion-reperfusion mice.

viable myocardium (Fig. 6). The thin segments were uniform in thickness and did not vary over the individual cross sections in a single heart by >10%. The average thicknesses of the thin segments were not different between hearts with permanent coronary artery occlusion (0.39 ± 0.036 mm; $n = 8$) and hearts reperfused after 2 h of occlusion (0.34 ± 0.032 mm; $n = 7$). In sham-operated mice, the thickness of the ventricular free wall was 0.84 ± 0.057 mm ($n = 9$).

We measured the endocardial area of the thin segment in each LV and examined this area as a function of the total surface area of the endocardium. Endocardial area underlying the thin segment divided by the total endocardial area of the LV was expressed as a percentage. The resulting value was referred to as the ventricular expansion ratio. For the reperfused group, the endocardial area of the thin segment was 7.8 ± 0.94 mm^2 ($n = 7$), which represented 12 ± 0.9% of the endocardial area. In the permanently occluded ventricles, the thin segment area was 11.1 ± 2.66 mm^2 ($n = 8$), which represented 18 ± 1.7% of the total endocardial area ($P < 0.05$ vs. reperfused). Because of the variation in thin segment size in the free wall of the ventricle, we elected to analyze the septal ventricular mass as well as the total noninfarcted ventricular mass. The measurement of the septum is not confounded by differential localization of ventricular myocytes in various portions of a free wall containing hypertrophied ventricle and papillary muscles. In addition, the septal mass is more remote from a variably sized ventricular expansion segment and may provide a better representation of compensatory hypertrophy resulting from increased ventricular stress.

Total noninfarcted ventricular mass in the sham-operated mice was 46.2 ± 3.28 mg ($n = 9$), and significant ventricular hypertrophy existed in the permanent occlusion mice (59.5 ± 4.34 mg; $P < 0.03$ vs. sham operated); reperfusion mice at 52.2 ± 2.42 mg were not significantly different from permanent occlusion or sham-operated mice. When the septal mass was separately evaluated, differences in the hypertrophic response between the permanently occluded and reperfused septum began to emerge. In comparison with the sham-operated ventricle (14.8 ± 0.99 mg), the reperfused ventricle showed modest septal hypertrophy (17.8 ± 1.10 mg), whereas there was greater septal mass (22.5 ± 1.08 mg) in the permanently occluded mice ($P < 0.002$ vs. reperfused and sham operated).

We hypothesized that the degree of septal hypertrophy represented a ventricular remodeling response to the greater mechanical disadvantage associated with the ventricular dilatation indicated by higher expansion ratios. This implied that septal mass would be a function of the endocardial surface area of the thin segment. The results of this analysis are shown in Fig. 7, and they appear to support our hypothesis. The five largest expansion ratios were all associated with ventricles with permanent occlusion; similarly, the greatest septal mass was associated with the permanently occluded ventricles. In the latter mice, the correlation between septal mass and expansion ratio is positive ($R = 0.85$, $P < 0.01$). Combined analysis of reperfused and permanently occluded mice did not significantly alter the slope with correlation ($R = 0.68$, $P < 0.01$), demonstrating that reperfusion did not change the relationship between septal hypertrophy and the expansion ratio. These anatomic data suggest that the nonreperfused ventricles tend to develop greater infarct expansion and compensatory hypertrophy.

DISCUSSION

The ability to treat the reperfused infarct directly suggests that there might be an opportunity to favorably influence tissue repair in the reperfused myocardial infarct, but a greater understanding of the variables associated with this process is necessary. Taking advantage of the ability to genetically manipulate the mouse, it may be possible to further clarify cellular and molecular mechanisms of tissue responses in the tissue repair after myocardial infarction. Mice with genetic deletions of adhesion molecules (24, 40), cytokines (20), and mast cells (46) have been developed and examined with respect to their effects on inflammatory fibrogenic influences.

We examined the physiological and related anatomic effects of late-reperfusion myocardial tissue remodeling in two types of myocardial infarction in the mouse. We considered release of occlusion at 2 h to be late because our studies concluded that this was the minimal coronary artery occlusion time necessary to produce infarcts equal to those seen with a permanent occlusion.

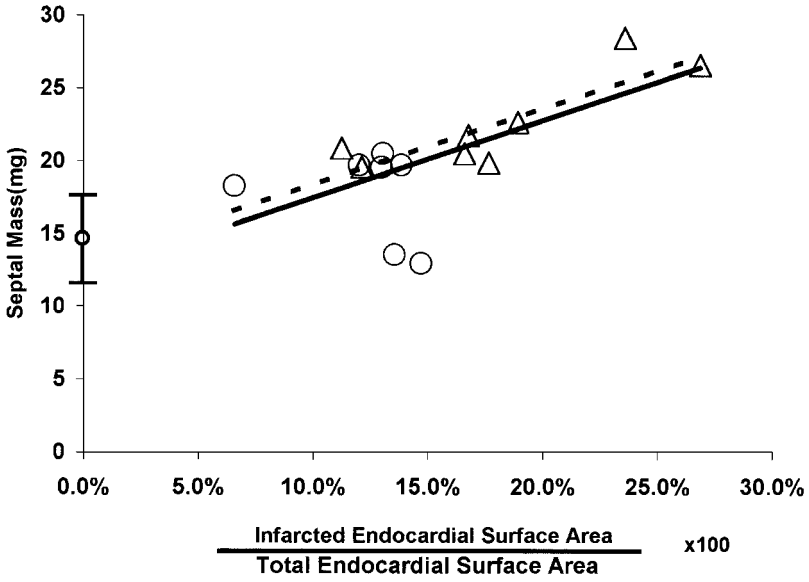

Fig. 7. Septal mass is plotted as a function of expansion ratio (length of thinned endocardial surface/total endocardial surface × 100). For permanent occlusion (△ and dotted line, $n = 8$), regression line was $y = ax + b$, $r = 0.85$, $P < 0.007$; for reperfusion (○, $n = 7$), there was inadequate distribution for regression analysis; for combined permanent occlusion and reperfusion (solid line) regression, $r = 0.675$, $P = 0.006$; ϕ = sham ± SD ($n = 9$).

Recently, functional and anatomic consequences of ventricular remodeling after permanent coronary artery occlusion in mice (30) and partial occlusion (23) were described. In the current study, we have elected to pursue both the physiological and the anatomic consequences of tissue repair in the presence and absence of reperfusion. To our knowledge, this represents the first attempt to characterize the effects of reperfusion on both the functional and anatomic consequences of cardiac remodeling in mice.

The protocol for permanent coronary occlusion and late reperfusion used in this study resulted in identical myocardial infarct size at 24 h. The functional studies demonstrated that basal ejection fraction was not different between the two groups. Despite the absence of significant differences in basal ejection fractions, both systolic and diastolic function of the permanently occluded ventricle were significantly impaired compared with either sham-operated or reperfused ventricles. In fact, after 2 wk following occlusion-reperfusion, abnormalities were not apparent in either systolic or diastolic function in the reperfused ventricles despite the fact that their mean ejection fraction was reduced by ~50% (see Fig. 4, *A* and *B*, and Fig. 5). These data suggest that the mice with permanent coronary occlusion acquired a functional handicap, in addition to the reduction in ejection fraction, that decreased their ability to adjust to unrelieved ischemic myocardial injury.

The anatomic data (Fig. 7) confirmed this mechanical disadvantage. The permanently occluded mice demonstrated both higher expansion ratios and greater compensatory ventricular hypertrophy than mice with reperfused infarcts. A highly significant correlation between the ventricular expansion ratio and the degree of septal hypertrophy was obtained, suggesting a positive relationship between the degree of ventricular hypertrophy and the area of dyskinetic myocardium. The relationship between these parameters did not appear to be a function of reperfusion; late reperfusion appeared to exert its effect by reducing ventricular expansion.

From a functional point of view, animals with greater hypertrophy and larger dyskinetic segments would be expected to have reduced ventricular compliance and reduction in ventricular filling velocity as demonstrated in Fig. 3. Similarly, reduction in aortic ejection velocity might result from mechanical disadvantages imposed by the thin segment or by the necessity for generating a higher preload to fill the less compliant ventricle.

In patients, survival of acute myocardial infarction after the initial hospital phase is largely dependent on residual ventricular function. Although reduction of myocardial infarct size after rapid reperfusion has become the hallmark of successful intervention, infarct size is not the only variable that affects postinfarct function. Ventricular unloading and inhibition of angiotensin II formation or signal transduction (which also unloads the ventricle) both modify resultant ventricular anatomy associated with infarction and ventricular repair (33, 39). Pfeffer and Braunwald (32) emphasized the prognostic importance of the geometric disadvantage associated with infarct expansion in patients.

Although the permanently occluded and the reperfused animals showed a similar reduction in ejection fraction, peak aortic flow velocity was decreased after 2 wk only in the permanently occluded group. LV ejection fraction is clearly dependent on infarct size (32), but the relationship between ejection fraction after infarction and maximum cardiac output or exercise capacity is not as clear. Franciosa et al. (7) described individuals with very low LV ejection fractions who were capable of very vigorous exertion. Similarly, peak aortic flow velocity and ejection fraction may vary independently. There are reports of overlap between peak aortic flow velocity values at rest for normal subjects and those with considerable heart disease, reduced ejection fractions, or experimental ischemia (16, 17, 26, 38). Peak aortic flow velocities for normal patients, and those with

coronary artery disease, diverged significantly in response to exercise or dipyridamole stress (22, 26). At the present time, we have not developed a satisfactory, standardized stress test for the highly labile mice used in the present study, but we would anticipate that stress might uncover ventricular dysfunction in the reperfused mice in a manner similar to that found by others (22, 26). Nevertheless, the data clearly demonstrate a more severe defect in both systolic and diastolic function in the permanently occluded animals evident even in the basal state.

In recent years, it has been recognized that reperfusion may have an effect on myocardial healing and ventricular anatomy beyond its ability to limit infarct size. Several clinical trials of thrombolytic therapy showed that late reperfusion reduces mortality (2, 15, 25, 29, 43, 45). Other clinical studies indicated that late reperfusion may reduce LV dilatation and remodeling (4, 18, 19, 42). Recent work (43) also suggested that the absence of a patent infarct vessel is associated with greater ventricular scar formation and ventricular remodeling observed by detecting collagen precursors circulating in the serum.

Several animal studies offer more detail on the role of reperfusion in ventricular remodeling. In the dog, late reperfusion resulted in accelerated inflammatory response and increased rate of effective infarct repair (35). Although the dog model did not manifest cardiac rupture or chronic infarct expansion as seen in human models, it was postulated that the acceleration of the early healing response would limit pathological remodeling (35). Similar studies done in rat suggested that late reperfusion limited infarct expansion (3). The extensive study by Boyle and Weisman (3) demonstrated that late reperfusion resulted in accelerated clearance of dead myofibrils and improved myocardial healing. Infarct expansion measured by the ratio of endocardial segment lengthening to infarct wall thinning was likewise reduced with reperfusion at both 7 and 21 days after myocardial infarction.

The factors associated with reperfusion that influence ventricular healing have not been carefully defined. Reperfusion in the first day may result in accelerated inflammatory responses that could favorably influence healing of the infarcted myocardium (5). Morita and co-workers (28) suggested that accelerated influx of monocytes results in increased monocyte-macrophage function that might favorably influence healing. Frangogiannis et al. (8) demonstrated that the reperfused myocardium manifests increased influx of mast cell precursors with resultant 5- to 10-fold increases of mast cell number in the healing infarct. Mast cells secrete histamine, basic fibroblast growth factor, and tryptase, all of which are potent fibrogenic agents (14, 31, 37). Frangogiannis and co-workers (8) demonstrated a high correlation between the presence of tissue mast cell and mitotically active myofibroblasts in the ventricle scar. In the final analysis, effective tissue repair requires effective removal of necrotic tissue, transition and ultimate suppression of the inflammatory response, myofibroblast influx, effective collagen formation, and ultimately, marked reduction in myofibroblast number. Optimal scar formation and ventricular topography are dependent on all of the above processes, and each is controlled in a complex manner.

In summary, the ability to manipulate postinfarct coronary blood flow in the mouse affords both functional and anatomic end points that can be followed in evaluating healing response to myocardial infarction in the presence and absence of reperfusion. Using mice with specific genetic manipulations may allow definition of the cellular and molecular factors associated with reperfusion-dependent improvement of ventricular healing and function.

The authors thank Damian Chaupin for assistance in computer analysis and Concepcion Mata and Sharon Malinowski for assistance in editing and preparation of the paper.

This work was supported by National Heart, Lung, and Blood Institute Grants HL-42550 and HL-22512, Proportional Technologies (HL-57086), Indus Instruments (HL-52364), the Medallion Foundation, and the DeBakey Heart Center.

Address for reprint requests and other correspondence: L. H. Michael, Baylor College of Medicine, Dept. of Medicine, Section of Cardiovascular Sciences, One Baylor Plaza, Houston, TX 77030-3498 (E-mail: lmichael@bcm.tmc.edu).

Received 1 November 1998; accepted in final form 20 March 1999.

REFERENCES

1. **Birdsall, H. H., D. M. Green, J. Trial, K. A. Youker, A. R. Burns, C. R. Mackay, G. J. LaRosa, H. K. Hawkins, C. W. Smith, L. H. Michael, M. L. Entman, and R. D. Rossen.** Complement C5a TGF-β1, and MCP-1, in sequence, induce migration of monocytes into ischemic canine myocardium within the first one to five hours after reperfusion. *Circulation* 95: 684–692, 1997.
2. **Bonaduce, D., M. Petretta, B. Villari, R. Breglio, G. Conforti, M. V. Montemurro, T. Lanzillo, and G. Morgano.** Effects of late administration of tissue-type plasminogen activator on left ventricular remodeling and function after myocardial infarction. *J. Am. Coll. Cardiol.* 16: 1561–1568, 1990.
3. **Boyle, M. P., and H. F. Weisman.** Limitation of infarct expansion and ventricular remodeling by late reperfusion. *Circulation* 88: 2872–2883, 1993.
4. **Dalen, J. E., J. M. Gore, E. Braunwald, J. Borer, R. J. Goldberg, E. R. Passamani, S. Forman, and G. Knatterud.** Six- and twelve-month follow-up of the phase I thrombolysis in myocardial infarction (TIMI) trial. *Am. J. Cardiol.* 62: 179–185, 1988.
5. **Entman, M. L., and C. W. Smith.** Post-reperfusion inflammation: a model of reaction to injury in cardiovascular disease. *Cardiovasc. Res.* 28: 1301–1311, 1994.
6. **Entman, M. L., K. A. Youker, T. Shoji, G. L. Kukielka, S. B. Shappell, A. A. Taylor, and C. W. Smith.** Neutrophil induced oxidative injury of cardiac myocytes: A compartmented system requiring CD11b/CD18-ICAM-1 adherence. *J. Clin. Invest.* 90: 1335–1345, 1992.
7. **Franciosa, J. A., M. Park, and T. B. Levine.** Lack of correlation between exercise capacity and indexes of resting left ventricular performance in heart failure. *Am. J. Cardiol.* 47: 33–39, 1981.
8. **Frangogiannis, N. G., M. L. Lindsey, L. H. Michael, K. A. Youker, R. B. Bressler, L. H. Mendoza, R. N. Spengler, C. W. Smith, and M. L. Entman.** Resident cardiac mast cells degranulate and release preformed TNF-α initiating the cytokine cascade in myocardial ischemia/reperfusion. *Circulation* 98: 699–710, 1998.
9. **Gruber, B. L., M. J. Marchese, and R. Kew.** Angiogenic factors stimulate mast-cell migration. *Blood* 86: 2498–2493, 1995.
10. **Hartley, C. J., J. L. Lacy, D. Dai, N. Nayak, G. E. Taffet, M. L. Entman, and L. H. Michael.** Functional cardiac imaging in mice using Ta-178. *Nat. Med.* 5: 237–239, 1999.

11. **Hartley, C. J., J. L. Lacy, J. Pocius, S. Daniel, E. Funk, G. E. Taffet, N. Nayak, M. L. Entman, and L. H. Michael.** Characterization of a murine model of heart failure by nuclear angiography (Abstract). *FASEB J*. 12: A407, 1998.
12. **Hartley, C. J., L. A. Latson, L. H. Michael, C. L. Seidel, R. M. Lewis, and M. L. Entman.** Doppler measurement of myocardial thickening with a single epicardial transducer. *Am. J. Physiol*. 245 (*Heart Circ. Physiol*. 14): H1066–H1072, 1983.
13. **Hartley, C. J., L. H. Michael, and M. L. Entman.** Noninvasive measurement of ascending aortic blood velocity in mice. *Am. J. Physiol*. 268 (*Heart Circ. Physiol*. 37): H499–H505, 1995.
14. **Heaney, L. G., L. J. Cross, C. F. Stanford, and M. Ennis.** Substance P induces histamine release from human pulmonary mast cells. *Clin. Exp. Allergy* 25: 179–186, 1995.
15. **Hirayama, A., T. Adachi, S. Asada, M. Mishima, S. Nanto, H. Kusuoka, K. Yamamoto, Y. Matsumura, M. Hori, M. Inoue, and K. Kodama.** Late reperfusion for acute myocardial infarction limits the dilatation of left ventricle without the reduction of infarct size. *Circulation* 88: 2565–2574, 1993.
16. **Isaaz, K., G. Ethevenot, P. Admant, B. Brembilla, and C. Pernot.** A new Doppler method of assessing left ventricular ejection force in chronic congestive heart failure. *Am. J. Cardiol*. 64: 81–87, 1989.
17. **Isaaz, K., G. Ethevenot, P. Admant, B. Brembilla, and C. Pernot.** A simplified normalized ejection phase index measured by Doppler echocardiography for the assessment of left ventricular performance. *Am. J. Cardiol*. 65: 1246–1251, 1990.
18. **ISIS (Second International Study of Infarct Survival) Collaborative Group.** Randomized trial of intravenous streptokinase, oral aspirin, both, or neither among 17,187 cases of suspected acute myocardial infarction: ISIS-2. *Lancet* 2: 349–360, 1989.
19. **Kennedy, J. W., J. L. Ritchie, K. B. Davis, M. L. Stadius, C. Maynard, and J. K. Fritz.** The Western Washington randomized trial of intracoronary streptokinase in acute myocardial infarction: a 12-month follow-up report. *N. Engl. J. Med*. 312: 1073–1078, 1985.
20. **Kubota, T., C. F. McTiernan, C. S. Frye, S. E. Slawson, A. P. Koretsky, A. J. Demetris, and A. M. Feldman.** Dilated cardiomyopathy in transgenic mice with cardiac specific overexpression of tumor necrosis factor-α. *Circ. Res*. 81: 627–635, 1998.
21. **Kumar, A. G., C. M. Ballantyne, L. H. Michael, G. L. Kukielka, K. A. Youker, M. L. Lindsey, H. K. Hawkins, H. H. Birdsall, C. R. Mackay, G. J. LaRosa, R. D. Rossen, C. W. Smith, and M. L. Entman.** Induction of monocyte chemoattractant protein-1 in the small veins of the ischemic and reperfused canine myocardium. *Circulation* 95: 693–700, 1997.
22. **Labovitz, A. J., A. C. Pearson, and B. R. Chaitman.** Doppler and two-dimensional echocardiographic assessment of left ventricular function before and after intravenous dipyridamole stress testing for detection of coronary artery disease. *Am. J. Cardiol*. 62: 1180–1185, 1988.
23. **Li, B., Q. Li, X. Wang, K. P. Jana, G. Redaelli, J. Kajstura, and P. Anversa.** Coronary constriction impairs cardiac function and induces myocardial damage and ventricular remodeling in mice. *Am. J. Physiol*. 273 (*Heart Circ. Physiol*. 42): H2508–H2519, 1997.
24. **Lu, H., C. W. Smith, J. Perrard, D. Bullard, L. Tang, S. B. Shappell, M. L. Entman, A. L. Beaudet, and C. M. Ballantyne.** LFA-1 is sufficient in mediating neutrophil emigration in Mac-1-deficient mice. *J. Clin. Invest*. 99: 1340–1350, 1997.
25. **Marino, P., L. Zanolla, and R. Zardini.** Effect of streptokinase on left ventricular modeling and function after myocardial infarction: the GISSI trial. *J. Am. Coll. Cardiol*. 14: 149–158, 1989.
26. **Mehdirad, A. A., G. A. Williams, A. J. Labovitz, R. J. Bryg, and B. R. Chaitman.** Evaluation of left ventricular function during upright exercise: correlation of exercise Doppler with postexercise two-dimensional echocardiographic results. *Circulation* 75: 413–419, 1987.
27. **Michael, L. H., M. L. Entman, C. J. Hartley, K. A. Youker, J. Zhu, S. R. Hall, H. K. Hawkins, K. Berens, and C. M. Ballantyne.** Myocardial ischemia and reperfusion: a murine model. *Am. J. Physiol*. 269 (*Heart Circ. Physiol*. 38): H2147–H2154, 1995.
28. **Morita, M., S. Kawashima, M. Ueno, A. Kubota, and T. Iwasaki.** Effects of late reperfusion on infarct expansion and infarct healing in conscious rats. *Am. J. Pathol*. 143: 419–430, 1993.
29. **Nidorf, S. M., S. C. Siu, G. Galambos, A. E. Weyman, and M. H. Picard.** Benefit of late coronary reperfusion on ventricular morphology and function after myocardial infarction. *J. Am. Coll. Cardiol*. 21: 683–691, 1993.
30. **Patten, R. D., M. J. Aronovitz, L. Deras-Mejia, N. G. Pandian, G. G. Hanak, J. J. Smith, M. E. Mendelsohn, and M. A. Konstam.** Ventricular remodeling in a mouse model of myocardial infarction. *Am. J. Physiol*. 274 (*Heart Circ. Physiol*. 43): H1812–H1820, 1998.
31. **Pennington, D. W., A. R. Lopez, P. S. Thomas, C. Peck, and W. M. Gold.** Dog mastocytoma cells produce transforming growth factor beta 1. *J. Clin. Invest*. 90: 35–41, 1992.
32. **Pfeffer, M. A., and E. Braunwald.** Ventricular remodeling after myocardial infarction. *Circulation* 81: 1161–1172, 1990.
33. **Pfeffer, M. A., J. M. Pfeffer, C. Steinberg, and P. Finn.** Survival after an experimental myocardial infarction: beneficial effects of long-term therapy with captopril. *Circulation* 72: 406–412, 1985.
34. **Pierce, G. F., T. A. Mustoe, J. Lingelbach, V. R. Masakowski, G. L. Griffin, R. M. Senior, and T. F. Deuel.** Platelet-derived growth factor and transforming growth factor-β enhance tissue repair activities by unique mechanisms. *J. Cell Biol*. 109: 429–440, 1989.
35. **Richard, V., C. E. Murry, and K. A. Reimer.** Healing of myocardial infarcts in dogs: effects of late reperfusion. *Circulation* 92: 1891–1901, 1995.
36. **Rizzo, V., and D. O. Defoux.** Mast cell activation accelerates the normal rate of angiogenesis in the chick chorioallantoic membrane. *Microvasc. Res*. 52: 245–257, 1996.
37. **Ruoss, S. J., T. Hartmann, and G. H. Caughey.** Mast cell tryptase is a mitogen for cultured fibroblasts. *J. Clin. Invest*. 88: 493–499, 1991.
38. **Sabbah, H. N., J. Przybylski, D. E. Albert, and P. D. Stein.** Peak aortic blood acceleration reflects the extent of left ventricular ischemic mass at risk. *Am. Heart J*. 113: 885–890, 1987.
39. **Schieffer, B., A. Wirger, M. Meybrunn, S. Seitz, J. Holtz, U. N. Riede, and H. Drexler.** Comparative effects of chronic angiotensin-converting enzyme inhibition and angiotensin II type 1 receptor blockage on cardiac remodeling after myocardial infarction in the rat. *Circulation* 89: 2273–2282, 1994.
40. **Sligh, J. E., Jr., C. M. Ballantyne, S. S. Rich, H. K. Hawkins, C. W. Smith, A. Bradley, and A. L. Beaudet.** Inflammatory and immune responses are impaired in ICAM-1 deficient mice. *Proc. Natl. Acad. Sci. USA* 90: 8529–8533, 1993.
41. **Taffet, G. E., C. J. Hartley, X. Wen, T. Pham, L. H. Michael, and M. L. Entman.** Noninvasive indexes of cardiac systolic and diastolic function in hyperthyroid and senescent mouse. *Am. J. Physiol*. 270 (*Heart Circ. Physiol*. 39): H2204–H2209, 1996.
42. **Topol, E. J., R. M. Califf, C. L. Grines, B. S. George, M. L. Sanz, T. Wall, M. O'Brien, M. Schwaiger, F. V. Aguirre, S. Young, J. J. Pompa, K. N. Sigmon, K. L. Lee, S. Ellis, and Thrombolysis and Angioplasty in Myocardial Infarction-6 Study Group.** A randomized trial of late reperfusion therapy for acute myocardial infarction. Thrombolysis and angioplasty in myocardial infarction-6 study group. *Circulation* 85: 2090–2099, 1992.
43. **Uusimaa, P., J. Risteli, M. Niemela, J. Lumme, M. Ikaheimo, A. Jounela, and K. Peuhkurinen.** Collagen scar formation after acute myocardial infarction: relationships to infarct size, left ventricular function, and coronary artery patency. *Circulation* 96: 2565–2572, 1997.
44. **Verani, M. S., J. L. Lacy, G. W. Guidry, S. Nishimura, J. J. Mahmarian, T. Athanasoulis, and R. Roberts.** Quantification of left ventricular performance during transient coronary occlusion at various anatomic sites in humans: a study using tantalum-178 and a multiwire gamma camera. *J. Am. Coll. Cardiol*. 19: 297–306, 1992.
45. **Villari, B., F. Piscione, D. Bonaduce, P. Golino, T. Lanzillo, M. Condorelli, and M. Chiariello.** Usefulness of late coronary thrombolysis (recombinant tissue-type plasminogen activator) in preserving left ventricular function in acute myocardial infarction. *Am. J. Cardiol*. 66: 1281–1286, 1990.
46. **Wershil, B. K., and S. J. Galli.** The analysis of mast cell function in vivo using mast cell-deficient mice. *Adv. Exp. Med. Biol*. 347: 39–54, 1994.